THERMODYNAMIC INVESTIGATIONS OF ZEOTROPIC MIXTURE OF R290, R23, AND R14 ON THREE-STAGE AUTO REFRIGERATING CASCADE SYSTEM

by

Mayilsamy SIVAKUMAR[a*] and Periasamy SOMASUNDARAM[b]

[a] Department of Basic Engineering, College of Fisheries Engineering, Tamil Nadu Fisheries University, Nagapattinam, Tamil Nadu, India
[b] Department of Automobile Engineering, Kongu Engineering College, Erode, Tamil Nadu, India

Original scientific paper
DOI: 10.2298/TSCI140103091S

The zeotropic mixture of environment friendly refrigerants (hydrocarbons and hydrofluorocarbons) being the only alternatives for working fluid in low temperature refrigeration system. Hence, three-stage auto refrigerating cascade system was studied for the existence using four combinations of three-component zeotropic mixture of six different refrigerants. The exergy analysis confirmed the existence of three-stage auto refrigerating cascade system. The performances of the system like coefficient of performance, exergy lost, exergic efficiency, efficiency defect, and the evaporating temperature achieved were investigated for different mass fractions in order to verify the effect of mass fraction on them. In accordance with the environmental issues and the process of sustainable development, the three-component zeotropic mixture of R290/R23/R14 with the mass fraction of 0.218:0.346:0.436 was performing better and hence can be suggested as an alternative refrigerant for three-stage auto refrigerating cascade system operating at very low evaporating temperature in the range of –97 °C (176 K), at coefficient of performance of 0.253 and comparatively increased exergic efficiency up to 16.3% (58.5%).

Key words: *zeotropic mixture of R290/R23/R14, coefficient of performance, three-stage auto refrigerating cascade, efficiency defect, exergy analysis and exergic efficiency*

Introduction

An unknown phenomenon (named later as Ozone Hole) has been for the first time measured by G. M. B Dobson in 1956. Ozone level in the Arctic region was 320 DU (Dobson units) or about 150 DU below normal value for spring time (about 450 DU). But the chlorofluorocarbons (CFC) lead the world of refrigeration industries for over six decades before the harmful effect on the ozone layer was identified in 1974 by Frank Sherwood Rowland and his postdoctoral associate Mario J. Molina.

Since exergic efficiency is higher in the case of system being charged 100%, coefficient of performance (COP) is highest at 50% charging and refrigerating effect is highest at 25% charging. Anand and Tyagi [1] suggested the system to be operated at optimum balance between refrigerating effect and energy savings.

Aprea and Maiorino [2] have studied *COP* improvement by employing pressure control at gas-cooler outlet, and quantified as 6.6-8.5% under minimum pressure working condition at different ambient temperature T_0.

* Corresponding author; e-mails: amsivakumar78@gmail.com, somuannauniv@hotmail.com

Cleland *et al.* [3] have quantified the system performances and stated that the system with mixture of propane and ethane (Care-50) reduced energy use by 6-8% under similar system cooling capacity relative to HCFC-22. With propane (Care-40) the energy use decreased by 5% but cooling capacity was 9% lower.

Sajjan *et al.* [4] have investigated the performance of the system of R22 with the retrofit of R407C. The experimental and theoretical investigation confirmed the drop in shell-and-tube condenser performance and quantified that the reduction in performance can be as large as 70% when compared to the full condenser load.

Jung *et al.* [5] have examined the performance of R290/R600a mixture of mass fraction 0.6:0.4 in domestic refrigerators and suggested the *COP* increase of 2.3%. Three to four percent of higher energy efficiency at faster cooling rate as well as shorter compressor on-time and lower compressor dome temperatures were confirmed with this mixture compared to R12.

Lemmon and Jacobsen [6] have reported that no additional parameters were required to model the ternary mixture and also slight systematic offsets were seen in several locations for example: the R32/125/134a system is unique from a modelling standpoint since it combines the three mixture equations, the individual equations for R32/125, R32/134a, and the generalized equation for R125/134a.

Gong *et al.* [8] have confirmed the new refrigeration cycle (NRC) having the evaporator circuit of two branches to realize Lorentz cycle with the advantage of temperature glide using the binary non-azeotropic refrigerant mixture (R32/R134a) which results in 8-9% *COP* raise and 9.5% increase in volumetric refrigerating capacity.

Yu *et al.* [7] achieved a minimum no-load temperature of –197.7 °C (about 75.7 K), –174 °C (about 99 K) was obtained at 110 W cooling capacities with the mixed-gases refrigeration using dual mixed-gases Joule-Thomson refrigeration system. They achieved the lowest temperature of –192 °C (about 81 K) with an effective preservation volume of 80 L at a relatively faster cooling-down rate in cryogenic chamber and found 2.5 hours to reach –180 °C, and 5 hours to reach –190 °C.

Johansson *et al.* [9] have found the charged composition and the circulated composition as well as the leak compositions differ. The differed compositions will not affect the cycle performance using the zeotropic mixtures like 407C. They have also suggested the predictive model to determine the circulating composition and suggested that this will be same for zeotropic mixtures consisting three or more components.

Du *et al.* [10] have suggested the use of zeotropic mixture of R134a and R23 of quality 0.7:0.3 as an alternate working fluid for auto refrigerating cascade (ARC) system to obtain high *COP*. They have also suggested that the raising of mass flux of high boiling liquid refrigerant and reducing the low boiling liquid refrigerant without any alteration in its discharge condition.

Lecompte *et al.* [11] found that the usage of mixtures results in an improvement of second law efficiency between 7.1% and 14.2% when compared to pure working fluids. The source of this improvement lies in a combination of a higher heat input and higher heat conversion efficiency and is mainly ascribed to decreased irreversibility in the condenser.

Sivakumar *et al.* [12-14] have suggested that the usage of three-component zeotropic mixture of environment friendly refrigerant mixtures work well within the three-stage ARC system reaching the lowest temperature of 176 K (–97 °C).

Atashafrooz *et al.* [15] used and conformed the usage of 2-D Cartesian for solving equations of conservation of mass, momentum, and energy with good consistency and acceptance of system parameters dealing with entropy generation.

Monsef *et al.* [16] have investigated the bubble pump with five horizontal tubes in low capacity absorption system of 2.5 kW capacity having submergence ratio 0.4. They confirmed the better performance in low capacity absorption refrigeration system.

Mani *et al.* [17] have developed mathematical models using design of experiments techniques and investigated the vapour compression refrigeration system. The mixture R290 and R600a of mass fraction 0.68:0.32 showed 10.7-23.6% higher *COP* than that with R12 and R134a. They confirmed the effective usage of HC mixtures as an alternate for vapour compression refrigeration system.

Fan *et al.* [18] have found that the mixture of CO_2 and dimethylether having suppressed flammability and explosive nature works efficiently as a refrigerant for heat pumps with a large heat-sink temperature rise. They found that the mixture of CO_2/dimethylether of mass fractions 0.28:0.72 and 0.03:0.97 can be used under conventional condensation pressure conditions and for space heating applications.

Even though the studies revealed many truth, these studies do not deal with ARC and its existence with respect to three-component zeotropic mixture. So this study is the stepping stone for the future in cryo-technologies.

Experimental set-up and procedure

The three-stage ARC system was fabricated as per the design parameters. The detailed photographic view of the system is shown in fig. 1, and the line diagram of the set-up is shown in fig. 2. The compressor used in this system is Kirloskar KCJ450LAL-B320. A four row air cooled condenser of 2TR (ton of refrigeration) capacity is used to facilitate the proper condensing area. An oil separator was connected to separate the oil from the compressor discharge and the separated oil was directed to the compressor doom through the suction line of the compressor.

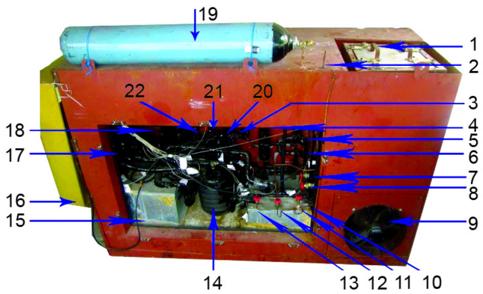

Figure 1. Photographic view of three-stage ARC system; *1 – evaporator tank with insulating lid, 2 – by-pass line with "T" connection, 3 – thermostatic expansion valve II, 4 – phase separator I, 5 – filter dryer, 6 – thermostatic expansion valve I, 7 – discharge line hand shut-off valve, 8 – suction line hand shut-off valve, 9 – outdoor unit with condenser fan, 10 – cascade condenser I, 11 – charging line, 12 – discharge line tap with hand shut-off valve, 13 – suction line tap with hand shut-off valve, 14 – pressure chamber, 15 – cascade condenser II, 16 – control unit with display unit, 17 – thermostatic expansion valve III, 18 – phase separator II, 19 – extra volume, 20 – NRV for RIII, 21 – NRV for RII, 22 – NRV for RI*

A no-return valve (NRV) is being used to avoid the back flow of the liquid refrigerant and ensuring the oil return into the compressor doom. Filter dryer is also used in the system after air cooled condenser for proper filtration and block free working of the system.

Since the pressure may go up to 4.826e+6 Pa during operation and 3.103e+6 Pa while system gets thermal equilibrium with atmosphere, a thick cylinder has been considered for phase separation. To ensure the proper working of the three-stage ARC system, an extruded Cu tube of 3 mm thickness with 0.4572 m and another of 0.3048 m height welded at top and bottom by 4 mm thick Cu plate were considered for phase separator I and phase separator II. Each separator is provided with one input line which penetrates until the bottom of the phase separator from the top. One more Cu line at the top of the separator provides the high

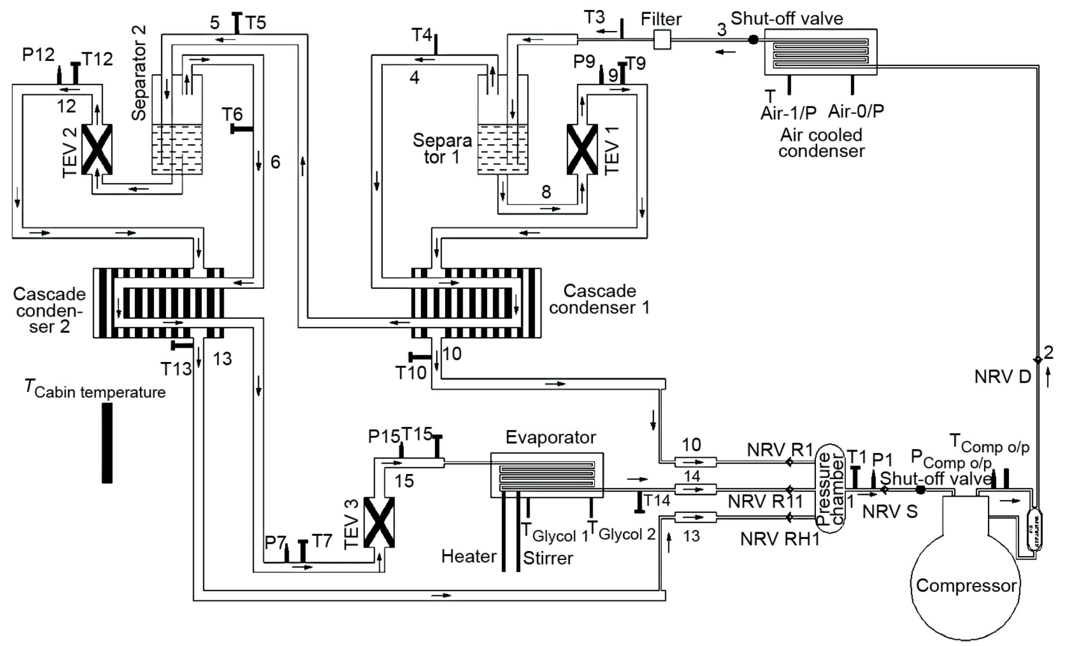

Figure 2. Line diagram of three-stage ARC system: flow path of refrigerant I in the circuit is 1-2-3-8-9-10-1; flow path of refrigerant II in the circuit is 1-2-3-4-5-11-12--13-1; flow path of refrigerant III in the circuit is 1-2-3-4-5-6-7-15-14-1; *1 – low pressure vapour of RI, RII, and RIII, 2 – high pressure – super-heated vapour of RI, RII, and RIII, 3 – sub-cooled liquid of RI + super-heated vapour of RII and RIII, 4 – super-heater vapour of RII and RIII, 5 – sub-cooled liquid of RII + super-heated vapour of RIII, 6 – super-heater vapour of RIII, 7 – sub-cooled liquid of RIII, 8 – sub-cooled liquid of RI, 9 – wet mixture of RI, 10 – super-heater vapour of RI, 11 – sub-cooled liquid of RII, 12 – wet mixture of RII, 13 – super-heater vapour of RII, 14 – super-heater vapour of RIII, 15 – wet mixture of RIII*

pressure line for the medium and low boiling refrigerants. The perfect utilization of the liquid refrigerant has been ensured by welding an output line right from the bottom of the phase separator. Combination of all three lines and the separator ensures perfect separation of liquid refrigerant through gravity separation.

The air cooled condenser must remove all the heat of refrigerants combined together and must condense the high boiling refrigerant which is the largest mass fraction of all three circulating refrigerants. In turn, it cools the medium boiling refrigerant and then the medium boiling refrigerant must cool the low boiling refrigerant to realize the circuit being working continuously. For the realization of these different requirements of each stage this three-stage ARC system considered the TES2:068Z3403 with orifice sizes of "1", "0", and "0X" decreasing continuously in size to accommodate the variation in cooling load.

The set-up has one tap with hand shut-off valve attached at the free end which can be extended using 0.0003302 m capillary of 3 m length from suction line. Another tap from high pressure line using 0.00635 m (1/4") line with hand shut-off valve attached at the free end which, in turn, can be connected through a "T" joint with the capillary and further with the provided extra volume in the low pressure side of the system. In case of the system pressure being large during thermal equilibrium with atmosphere after switching off, these two extensions can be used as by-pass line for equalizing the high and low pressure side of three-stage ARC system before starting the compressor.

The capillary will be useful in slow and study suction during start-up of the compressor without any sudden loading of the compressor while the discharge tap valve being closed from the extra volume. The system is provided with one more tap with hand shut-off valve at the free end which will be very useful in the case of refrigerant charging while system is working continuously with its operation.

Cascade condensers I and II are used as counter-flow heat exchangers for the better and efficient heat transfer performance between the refrigerants flowing in the circuit. Since the heat rejected by the low boiling refrigerant must be equal to the heat gained by the medium boiling refrigerant at cascade condenser II, heat rejected by the mixture of medium and low boiling refrigerants should be equal to heat gained by the high boiling refrigerant in cascade condenser I. Cascade condensers were insulated with 100 mm thick polyurethane foam (PUF) around them by a bounding box. Flow of hot fluid inside the inner tube ensures the heat transferred to the cold fluid flowing in outer tube of cascade condenser in both the cases.

A pressure chamber is used to provide extra volume as well as mixing chamber at suction side of the system through three different NRV from evaporator I (outlet of cascade condenser I outer tube, cold fluid – high-boiling refrigerant), evaporator II (outlet of cascade condenser II outer tube, cold fluid – medium-boiling refrigerant), and evaporator III (low-boiling refrigerant). This ensures that the problem of high-, medium-, and low-boiling refrigerants influencing on pressure build-up on each other during operation is resolved.

Outdoor unit of the system is provided with two hand shut-off valves at both the ends along its line for refrigerant isolation and retrieval of refrigerants in case of any alteration work and trials.

The system was equipped with two separate energy meters (kWh) to indicate the power consumption of the compressor and the heat load given to the evaporator. The heater was connected through on-off control.

Twelve SZ-7505-P type RTD sensors with an accuracy of ±1 °C, and around thirteen Mars DTI-204 type 3 wire RTD sensors with ±1 °C were connected at different positions as stated by the state points of the system. A total of six number of WIKA 213.53.63 (0-100 kg/cm^2) pressure gauges were used in this system for continuous monitoring of system pressure at suction and discharge side. The readings confirm that no considerable variation along the length of the piping. So it was decided to use individual suction pressure for each refrigerant after each expansion, similarly discharge pressure at the end of the high pressure line of low boiling refrigerant, which travels greater distance from the compressor, just before thermostatic expansion valve (TEV) III. Thermo wells were set for mounting the temperature sensors with ethylene glycol and water mixture of 0.5:0.5 ratios. This being a slow and time consuming process, the sensors were set directly on the Cu piping as like the bulb of the thermostatic expansion valves ensuring fast and instant response of the temperature sensors.

A heater was used to provide load to the evaporator. A stirrer was also used to enhance the heat transfer in the secondary fluid in the evaporator tank. Evaporator tank was insulated with 150 mm PUF insulation around it. The perfect insulation is being ensured inside the evaporator tank. The total heat leak in the set-up was less than 5% of the total evaporator load.

Refrigerant charging

The ARC system was subjected to leak test with nitrogen at 3.172e+6 Pa. The system was kept idle for 60 hours and checked for pressure drop to ensure zero leak. Then the system was evacuated to the vacuum level. After completing the evacuation test, the system was ready for charging the refrigerant mixture. Initially, low-boiling refrigerant was charged through charging valve followed by medium-boiling refrigerant, and then by the low-boiling refrigerant as per the thermodynamically correct mass fraction. A digital mass balance was used to have accurate mass of charged quantity.

Testing methodology

After charging the mixture with desired mass fraction, the system was started with uniform ambient temperature. Before starting the system, pressures at discharge side and suction side were equalized by the use of the by-pass line and extra volume to ensure less starting torque of the compressor. After the starting of compressor the valve was closed. Different observations, like temperatures at each state point, pressures at each state point, power consumption of compressor, and evaporator heat load were recorded. All the observations were made after getting the equilibrium condition of the system. The equilibrium state was arrived by adjusting the heater load and evaporator refrigerating effect. The unchanged temperature of secondary medium ensured this equilibrium state.

The total mass of the refrigerant mixture and mass fraction of mixture was varied and the performance was recorded. This procedure was repeated for different mass fractions. All the parameters of the system and mainly the power consumption were observed after the system has reached the steady-state condition. Values obtained were used for this study and the characteristic curves were plotted and the performance of ARC system was studied.

Heat leak test

The heat leak test was carried out to find heat infiltration into the evaporator tank from ambient temperature and different secondary fluid temperatures. Initially the temperature of secondary fluid in the evaporator tank was brought down and then the system was stopped. Then the time taken for every one-degree increment of secondary fluid temperature was recorded.

The NRV connected at the end of the evaporator coil ensured no influence of back flow of refrigerant that would heat the secondary fluid. The heat infiltration was calculated using the equation:

$$\text{Calorimeter heat gain} = \frac{m c_p \Delta T}{\Delta t}$$

where m [kg] is the total mass of secondary fluid in the evaporator tank, c_p [kJkg^{-1}K^{-1}] – the specific heat of secondary fluid, ΔT – [°C] the difference of initial and final temperature, and Δt – [second] the time taken for ΔT increase of temperature.

The calculated amount of evaporator heat infiltration for particular secondary fluid temperature was added to the load indicated in the wattmeter. Hence, the exact load on evaporator was estimated.

Exergy analysis

This investigation performs an exergy analysis to make all exergy losses visible in the process under study. The method is very powerful when comparing two or more solutions in an objective and quantitative manner. Exergy analysis is especially useful in the design phase and during optimization of new processes in terms of exact location for improvement by giving the best clues where to start, namely at the point where the largest exergy losses appear but does not give direct answers on how to improve the efficiency of the process. Under the assumption that the change of kinetic and potential energy is negligible and the ambient temperature is T_0, the exergy is given by:

$$\psi = h - T_0 s \tag{1}$$

$$\psi = (h - h_0) - T_0 (s - s_0) \tag{2}$$

For the three-stage ARC system the component wise the exergy balance equation can be written:

(a) For compressor; the exergy loss (due to irreversibility) in the compressor:

$$I_{\text{comp}} = \dot{m}(h_1 - T_0 s_1) + w_c - \dot{m}(h_2 - T_0 s_2) \tag{3}$$

(b) For air-cooled condenser; the exergy loss (due to irreversibility) in the air-cooled condenser:

$$I_{\text{ACC}} = \dot{m}(h_2 - T_0 s_2) - \dot{m}(h_3 - T_0 s_3) - Q_{\text{ACC}}\left(1 - \frac{T_0}{T_{\text{ACC}}}\right) \tag{4}$$

(c) For condenser I (cascade condenser I: hot fluid flow); the exergy loss (due to irreversibility) in the condenser I:

$$I_{\text{condenser I}} = \dot{m}_{\text{RII+RIII}}(h_4 - T_0 s_4) - \dot{m}_{\text{RII+RIII}}(h_5 - T_0 s_5) - Q_{\text{condenser I}}\left(1 - \frac{T_0}{T_{\text{condenser I}}}\right) \tag{5}$$

(d) For condenser II (cascade condenser II: hot fluid flow); the exergy loss (due to irreversibility) in the condenser II:

$$I_{\text{condenser II}} = \dot{m}_{\text{RIII}}(h_6 - T_0 s_6) - \dot{m}_{\text{RIII}}(h_7 - T_0 s_7) - Q_{\text{condenser II}}\left(1 - \frac{T_0}{T_{\text{condenser II}}}\right) \tag{6}$$

(e) For thermostatic expansion valve – I; the exergy loss (due to irreversibility) in the thermostatic expansion valve I:

$$I_{\text{TEV I}} = \dot{m}_{\text{RIII}} T_0 (s_9 - s_8) \tag{7}$$

(f) For thermostatic expansion valve II; the exergy loss (due to irreversibility) in the thermostatic expansion valve I:

$$I_{\text{TEV II}} = \dot{m}_{\text{RII}} T_0 (s_{12} - s_{11}) \tag{8}$$

(g) For thermostatic expansion valve III; the exergy loss (due to irreversibility) in the thermostatic expansion valve I:

$$I_{\text{TEV III}} = \dot{m}_{\text{RIII}} T_0 (s_{15} - s_7) \tag{9}$$

(h) For evaporator III; the exergy loss (due to irreversibility) in the evaporator III:

$$I_{\text{evaporator III}} = \dot{m}_{\text{RIII}}(h_{15} - T_0 s_{15}) + Q_{\text{evaporator III}}\left(1 - \frac{T_0}{T_{\text{evaporator III}}}\right) - \dot{m}_{\text{RIII}}(h_{14} - T_0 s_{14}) \tag{10}$$

(i) For evaporator II (cascade condenser II: cold fluid flow); the exergy loss (due to irreversibility) in the evaporator II:

$$I_{\text{evaporator II}} = \dot{m}_{\text{RII}}(h_{12} - T_0 s_{12}) + Q_{\text{evaporator II}}\left(1 - \frac{T_0}{T_{\text{evaporator II}}}\right) - \dot{m}_{\text{RII}}(h_{13} - T_0 s_{13}) \tag{11}$$

(j) For evaporator I (cascade condenser I: cold fluid flow); the exergy loss (due to irreversibility) in the evaporator I:

$$I_{\text{evaporator I}} = \dot{m}_{\text{RI}}(h_9 - T_0 s_9) + Q_{\text{evaporator I}}\left(1 - \frac{T_0}{T_{\text{evaporator I}}}\right) - \dot{m}_{\text{RI}}(h_{10} - T_0 s_{10}) \tag{12}$$

The total exergy loss of the system is given by the correlation:

$$I_{\text{total}} = I_{\text{comp}} + I_{\text{ACC}} + I_{\text{condenser I}} + I_{\text{condenser II}} + I_{\text{evaporator I}} + I_{\text{evaporator II}} + I_{\text{evaporator III}} + \\ + I_{\text{TEV I}} + I_{\text{TEV II}} + I_{\text{TEV III}} \tag{13}$$

The exergy efficiency is given by:

$$\eta_x = \frac{\psi_1 - \psi_{14}}{w_c} = \frac{Q_{\text{evaporator III}}\left(1 - \dfrac{T_0}{T_{\text{evaporator III}}}\right)}{w_c} \tag{14}$$

For the three-stage ARC system the component wise efficiency defect, δ_i, considering the ratio of exergy used in the corresponding component, ψ_i, to the exergy required to sustain the process (exergy through the compressor, w_c):

$$\delta_i = \frac{\psi_i}{w_c} \tag{15}$$

The overall performance of the three-stage ARC system is determined by evaluating its *COP,* and is calculated as the ratio between the refrigerating capacity, $Q_{\text{evaporator III}}$, and the electrical power supplied to the compressor, w_c:

$$COP = \frac{Q_{\text{evaporator III}}}{w_c} \tag{16}$$

Results and discussions

The values of *COP*, exergy lost, exergic efficiency, and efficiency defect readings in individual components were calculated using the readings obtained by the experimental set-up. These parameters were discussed in this section for better understanding of the three-stage ARC system.

Figure 3 shows the variation of *COP* with the variation of mass fraction of R290 and R14 in the zeotropic mixture of R290, R23, and R14. It is observed that the decrease in *COP* is due to the increase in mass flow through the system and through the compressor which increases the compressor work and which in turn reduces the *COP*. Figure 3 also explains the concept of slight increase in *COP* for the higher mass ratio of R290 and lower mass ratio of

R14 due to the higher flow rate of high boiling refrigerant which ensures the proper cooling and effectiveness in the first stage itself which in turn adds a slight increment in refrigerating effect and thus the *COP*. The maximum and minimum value of *COP* observed are 0.340 for the mixture of R290, R23, and R14 with the mass fraction of 0.158:0.346:0.496, and 0.253 for the mass fraction of 0.218:0.346:0.436.

The maximum value of exergic efficiency from the fig. 3 was 50.3% which corresponds to the mixture of R290, R23, and R14 with the mass fraction of 0.158:0.346:0.496, and the lowest among the values obtained is 35.9% which corresponds to the mixture of R290, R23, and R14 with the mass fraction of 0.278:0.346:0.376. The gradual increase in exergic efficiency of the mixture is noted with increase in quantity of R290 and drastically decreases after the optimum ratio along the course of operation. The trend of exergy efficiency may be noted due to the proper heat transfer between refrigerants in cascade condensers and thus the increase in refrigerating effect which in turn gives better efficiencies and it drastically reduces due to the excess amount of refrigerant flow with higher value of terminal velocity, which will not be able to efficiently transfer the heat between the refrigerants in cascade condensers.

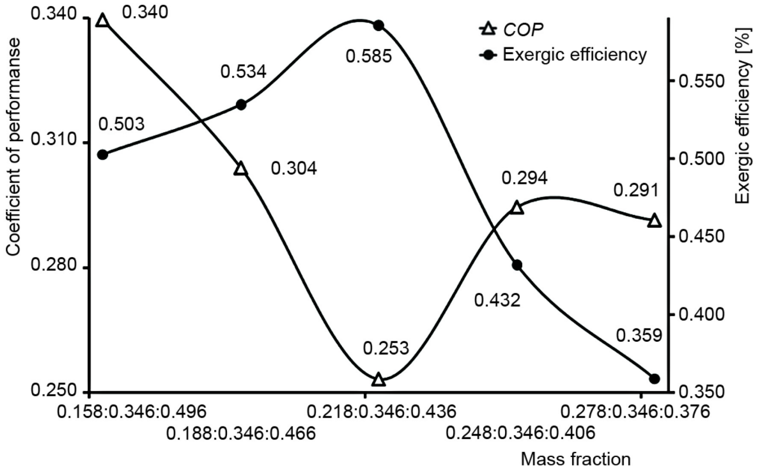

Figure 3. Variation of *COP* and exergic efficiency for different mass fraction of R290 and R14 in the zeotropic mixture of R290, R23, and R14

Figure 4 shows the variation of evaporating temperatures and *COP* achieved using the zeotropic mixture, during different trials with the variation of mass fractions of R290, R23, and R14. The lower most evaporating temperature achieved is 176 K (–97 °C) which corresponds to the mixture of R290, R23, and R14 with the mass fraction of 0.218:0.346:0.436 with *COP* of 0.253 and the evaporating temperature achieved is 186 K (–87 °C) which correspond the mass fraction 0.158:0.346:0.496 and 0.278:0.346:0.376 with *COP* 0.503 and 0.359.

Even though the *COP* is higher in case of mass fraction trials 0.158:0.346:0.496, 0.188:0.346:0.466, 0.248:0.346:0.406, and 0.278:0.346:0.376, the evaporating temperatures achieved during these trials are higher. So the interpretations of this work can lean towards the lesser *COP* with lower evaporating temperature trials. Hence the interpretations of this work can lean towards the lesser *COP* with lower evaporating temperature trials.

Figure 5 shows the variation of evaporating temperature and refrigerating effect with the variation of mass fraction of R290 and R14 in the zeotropic mixture of R290, R23, and R14. Even though the higher mass flow of high boiling refrigerant enable sufficient cooling

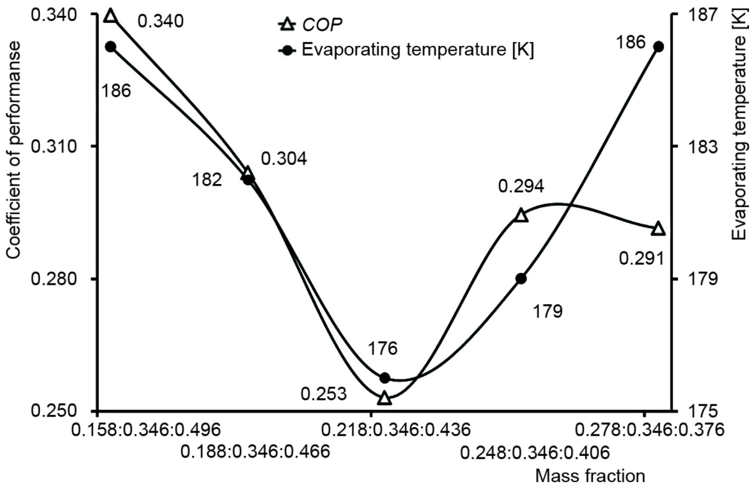

Figure 4. Variation of *COP* and evaporating temperature for different mass fraction of R290 and R14 in the zeotropic mixture of R290, R23, and R14

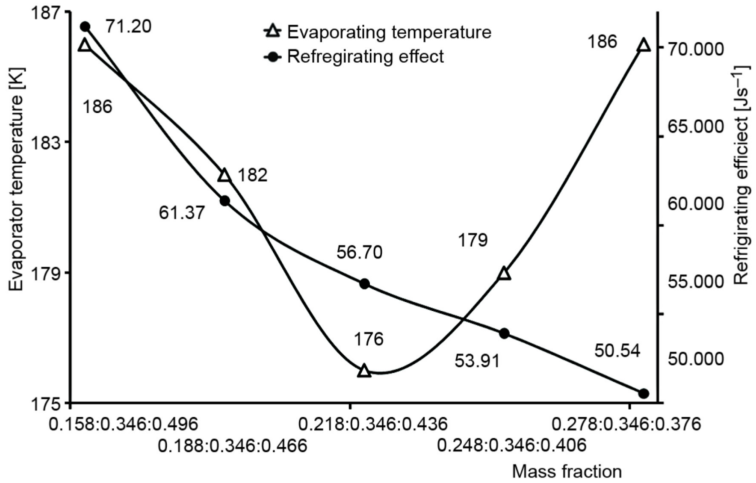

Figure 5. Variation of evaporating temperature and refrigerating effect for different mass fraction of R290 and R14 in the zeotropic mixture of R290, R23, and R14

for medium and low boiling refrigerant in condenser I, the decreased mass flow rate of the low boiling refrigerant at evaporator III with higher terminal velocity reduces the refrigerating effect at lower evaporating temperatures. The higher values of refrigerating effect is due to the increased mass flow of low boiling refrigerant assisting with less amount of compressor work and thus the higher *COP*. The higher and lower values of refrigerating effect achieved during the trials are 71.2 W and 50.54 W which correspond to the zeotropic mixtures of mass fractions 0.158:0.346:0.496 and 0.278:0.346:0.376.

Figure 5 interprets the highest value of refrigerating effect and its corresponding higher evaporating temperature which is not desirable in case of refrigerating cycle. So the optimum solution should be between the lowest evaporating temperature and optimum refrigerating effect.

Figure 6 shows the variation of compressor work input with the variation of mass fraction of R290 and R14 in the zeotropic mixture of R290, R23, and R14. The maximum and minimum values of these trials are 209.65 W and 173.44 W, corresponding to the mixtures of mass fractions 0.158:0.346:0.496 and 0.278:0.346:0.376. The trend of reduction of compressor work after the optimum increase in mass flow of high boiling refrigerant is reached, it is observed during the trials due to the reduced mass flow of low boiling high density refrigerant which has greater influence on compressor work has better *COP* due to the increased mass flow of high boiling refrigerant which can be easily compressed and thus the compressor work reduces.

As the compressor work should be minimum at lowest evaporating temperatures, the fig. 6 does not suggest the trial 5 with mass fraction 0.278:0.346:0.376. So it can be interpreted that the optimum between evaporating temperature and compressor work.

Figure 7 shows the variation of compressor work and exergy lost at compressor with the variation of mass fraction of R290 and R14 in the zeotropic mixture of R290, R23, and R14. The maximum and minimum values of exergy lost at compressor are 143.43 W and 209.65 W, corresponding to the mixture of mass fraction 0.158:0.346:0.496 having the value of 155.9 W of compressor work input, and 0.278:0.346:0.376 having the value of 173.44 W of compressor work input. It is evident that whenever the temperature difference between the two-state points is high, the exergy lost (change in entropy is also high which in turn the exergy or less availability) is also high.

Even though high compressor work leads to lesser *COP* and low compressor work to higher *COP* through the linear variation of exergy loss, this system performs little different

Figure 6. Variation of evaporating temperature and compressor work input for different mass fraction of R290 and R14 in the zeotropic mixture of R290, R23, and R14

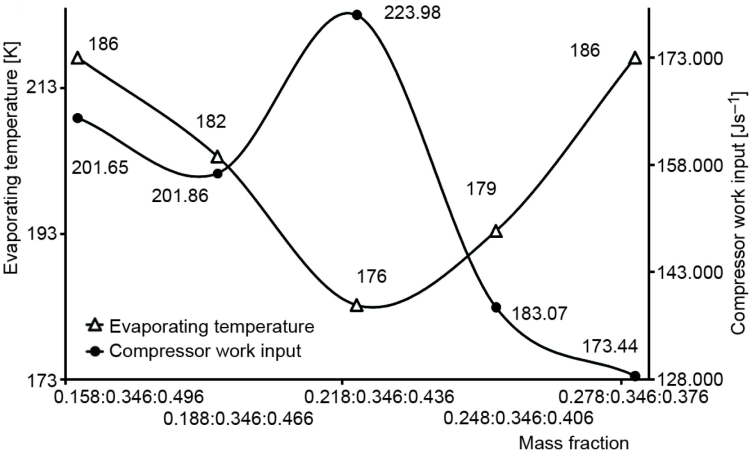

Figure 7. Variation of compressor work input and exergy lost in compressor for different mass fraction of R290 and R14 in the zeotropic mixture of R290, R23, and R14

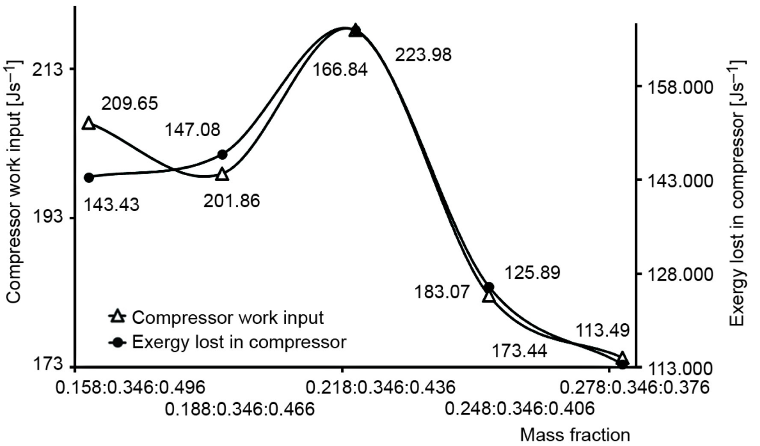

due to the mixing of low boiling high density and high boiling low density refrigerants which will increase the *COP* at both the cases. The optimum of compressor work and exergy lost can be the solution.

Figure 8 shows the variation of evaporating temperatures achieved using the zeotropic mixture during the different trials with the variation of mass fractions of R290, R23, and R14. The lower most evaporating temperature achieved is 176 K (–97 °C) which corresponds to the mixture of R290, R23, and R14 with the mass fraction of 0.218:0.346:0.436, and the evaporating temperature achieved is 186 K (–87 °C) which corresponds with the mass fraction 0.158:0.346:0.496, and 0.278:0.346:0.376. The trend of increase in evaporating temperature was due to increased mass flow of low boiling refrigerant for the trials 4 and 5. The increase in evaporating temperature was due to the insufficient mass flow of high boiling refrigerant which should cool the medium and low boiling refrigerants during trials 1 and 2.

Figure 9 shows the variation of efficiency defect in each component of the ARC system with the variation of mass fraction of R290 and R14 in the zeotropic mixture of R290, R23, and R14. The maximum and minimum exergy defect are found at compressor (0.68,

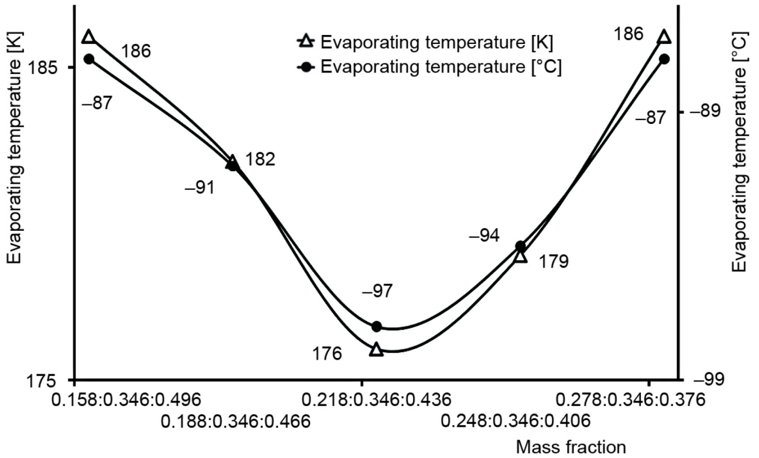

Figure 8. Variation of evaporating temperature for different mass fraction of R290 and R14 in the zeotropic mixture of R290, R23, and R14

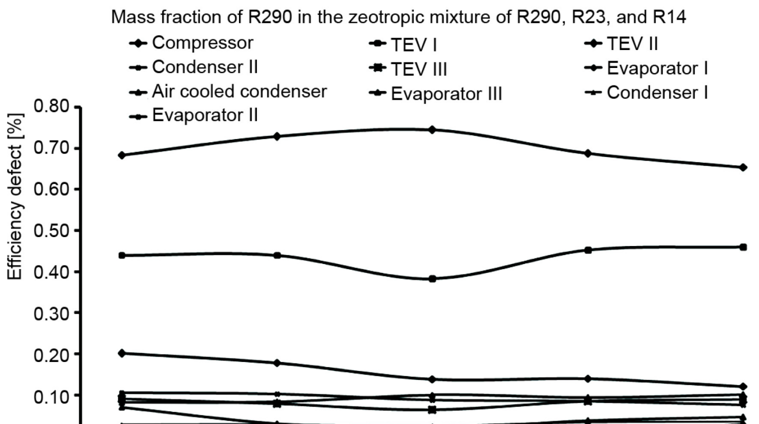

Figure 9. Variation of efficiency defect in each component of ARC system for different mass fraction of R290 and R14 in the zeotropic mixture of R290, R23, and R14

0.73, 0.74, 0.69, and 0.65, corresponding to trials 1, 2, 3, 4, and 5), and at evaporator II (0.02, 0.00, 0.00, 0.02, and 0.02, corresponding to trials 1, 2, 3, 4, and 5).

The phenomenon of increase in efficiency defect is observed due to greater losses in compressor during trials 1, 2, and 3 with increased mass flow of high boiling refrigerant which has the tendency to be easily compressed and the excess energy available creates excess temperature difference and thus the exergy loss and also the efficiency defect. On the other hand the excess amount of work input during the trials 4 and 5 with the mass fraction of 0.248:0.346:0.406, and 0.278:0.346:0.376 are utilized to compress the low boiling high density refrigerants which make sure less amount of temperature raise during operation and thus the lesser exergy losses when compared to the trials of 1, 2, and 3 in each and every component.

Figures 1-9 interpret that the three-stage ARC system is efficient in dealing with the low temperature at the range of 176 K (–97 °C) with the area of improvement or concentration should be on the compressor in the aspect of exergy loss and performance improvement of any ARC system.

Conclusions

Exergic analysis and performance analysis of three-stage ARC system was conducted on the set-up operating either between the evaporation and condensation temperatures of 176 K (–97 °C) and 301 K (30 °C) or over the temperature range of 187 °C. With reference to the exergic and experimental study of the system the following conclusions were made.

- The zeotropic mixture of R290/R23/R14 with the mass fraction of 0.218:0.346:0.436 having *COP* of 0.253 and 58.5% of exergic efficiency was recommended as an alternative refrigerant for three-stage ARC system working at the temperature range of 176 K (–97 °C).
- The overall efficiency defect is found to be at the range of 65 and 75 for the mixture of R290/R23/R14 with the mass fraction of 0.218:0.346:0.436.
- The highest efficiency defect was found to be at compressor and thus area of improvement lies in compressor. Following is the order of components which has larger efficiency defect. They are compressor TEV and condensers.
- The highest exergic efficiency was found to be 58.5% for the zeotropic mixture of R290/R23/R14 with the mass fraction of 0.218:0.346:0.436 operating at the temperature range of 176 K (–97 °C).
- In general, the the zeotropic mixture of R290/R23/R14 with the mass fraction of 0.218:0.346:0.436 having *COP* of 0.253 and 58.5% of exergic efficiency was working well in the three-stage ARC system.

Thus it can be concluded that the zeotropic mixture of R290/R23/R14 with the mass fraction 0.218:0.346:0.436 as an alternative refrigerant for three-stage ARC system with slight modification of the system.

Nomenclature

COP – coefficient of performance
h – specific enthalpy, [Jkg^{-1}]
I – exergy loss, [Js^{-1}]
$\dot{m}$ – mass (total refrigerant) flow rate (= $m_{RI} + m_{RII} + m_{RIII}$), [$kgs^{-1}$]
m_R – mass flow rate of a refrigerant, [kgs^{-1}]
Q – heat removed at air cooled condenser or evaporator, [W]
s – specific entropy, [$Jkg^{-1}K^{-1}$]
T_0 – ambient temperature, [K]
$T_{condenser}$ – condensing temperature (refrigerant), [K]
$T_{evaporator}$ – evaporating temperature of cascade condenser (refrigerant), [K]
w_c – compressor work input, [W]

Greek symbols

δ – efficiency defect
ψ – exergy flow, [Jkg^{-1}]
η_x – exergy efficiency, [%]

Subscripts

TEV – thermostatic expansion valve
ACC – air cooled condenser
R – refrigerant
1,…, 15 – state points of the system

References

[1] Anand, S., Tyagi, S. K., Exergy Analysis and Experimental Study of a Vapour Compression Refrigeration Cycle, *Journal of Thermal Analysis and Calorimetry*, *110* (2012), 2, pp. 961-971
[2] Aprea, C., Maiorino, A., Heat Rejection Pressure Optimization for a Carbon Dioxide Split System: An Experimental Study, *Applied Energy*, *86* (2009), 11, pp. 2373-2380
[3] Cleland, D. J., *et al.*, Use of Hydrocarbons as Drop-in Replacements for HCFC-22 in on Farm Milk Cooling Equipment, *International Journal of Refrigeration*, *32* (2009), 6, pp. 1403-1411
[4] Sajjan, D., *et al.*, Reasons for Drop in Shell-and-Tube Condenser Performance when Replacing R22 with Zeotropic Mixtures. Part 1: Analysis of Experimental Findings, *International Journal of Refrigeration*, *27* (2004), 5, pp. 552-560
[5] Jung, D., *et al.,* Testing of Propane/Isobutane Mixture in Domestic Refrigerators, *International Journal of Refrigeration*, *23* (2000), 7, pp. 517-527
[6] Lemmon, E. W., Jacobsen, T. R., Equations of State for Mixtures of R-32, R-125, R-134a, R-143a, and R-152a, *Journal of Physical Chemical Reference Data*, *33* (2004), 2, pp. 592-620
[7] Gong, M., *et al.*, Development of a –186 °C Cryogenic Preservation Chamber Based on a Dual Mixed-Gases Joule-Thomson Refrigeration Cycle, *Applied Thermal Engineering*, *36* (2012), Apr., pp. 188-192
[8] Yu, J., *et al.*, Application of an Ejector in Autocascade Refrigeration Cycle for the Performance Improvement, *International Journal of Refrigeration*, *31* (2008), 2, pp. 279-286
[9] Johansson, A., Lundqvist, P., A Method to Estimate the Circulated Composition in Refrigeration and Heat Pump Systems using Zeotropic Refrigerant Mixtures, *International Journal of Refrigeration*, *24* (2001), 8, pp. 798-808
[10] Du, K., *et al.*, A Study on the Cycle Characteristics of an Auto-Cascade Refrigeration System, *Experimental Thermal and Fluid Science*, *33* (2009), 2, pp. 240-245
[11] Lecompte, S., *et al.*, Exergy Analysis of Zeotropic Mixtures as Working Fluids in Organic Rankine Cycles, *Energy Conversion and Management*, *85* (2014), Sept., pp. 727-739
[12] Sivakumar, M., *et al.*, Exergy and Energy Analysis of Three Stage Auto Refrigerating Cascade System Using Zeotropic Mixture for Sustainable Development, *Energy Conservation and Management, 84* (2014), Aug., pp. 589-596
[13] Sivakumar, M., *et al.*, Exergy and Performance Analysis of Three Stage Auto Refrigerating Cascade (3 stage ARC) System Using Zeotropic Mixture of Eco-Friendly Refrigerants, *International Review of Mechanical Engineering, 8* (2014), 1, pp. 124-134
[14] Sivakumar, M., *et al.*, Exergy and Performance Analysis of Three Stage Auto Refrigerating Cascade (3 stage ARC) System Using Environment Friendly Zeotropic Mixture of R290, R170, and R14, *Pollution Research, 32* (2013), 4, pp. 943-952
[15] Atashafrooz, M., *et al.*, Numerical Investigation of Entropy Generation in Laminar Forced Convection Flow over Inclined Backward and Forward Facing Steps in a Duct Under Bleeding Condition, *Thermal Science, 18* (2014), 2, pp. 479-492
[16] Monsef, H., *et al.*, Design and Construction of a Low Capacity Pump-Less Absorption System, *Thermal Science, 18* (2014), 2, pp. 577-590
[17] Mani, K., *et al.*, Experimental Investigations with Eco-Friendly Refrigerants Using Design of Experiments Technique – Mathematical Modelling and Experimental Validation, *Thermal Science, 18* (2014), Suppl. 2, pp. S363-S374
[18] Fan, X. W., *et al.*, Theoretical Study of Heat Pump System Using CO_2/Dimethylether as Refrigerant, *Thermal Science, 17* (2013), 5, pp. 1261-1268

Paper submitted: January 3, 2014
Paper revised: June 25, 2014
Paper accepted: July 12, 2014